Cell Reports, Volume *37*

Supplemental information

Combined whole-organ imaging at single-cell resolution and immunohistochemical analysis of prostate cancer and its liver and brain metastases

Julian Taranda, Grinu Mathew, Kaitlin Watrud, Nour El-Amine, Matthew F. Lee, Corey Elowsky, Anastasiia Bludova, Sintia Escobar Avelar, Dawid G. Nowak, Tse-Luen Wee, John E. Wilkinson, Lloyd C. Trotman, and Pavel Osten

Figure S1

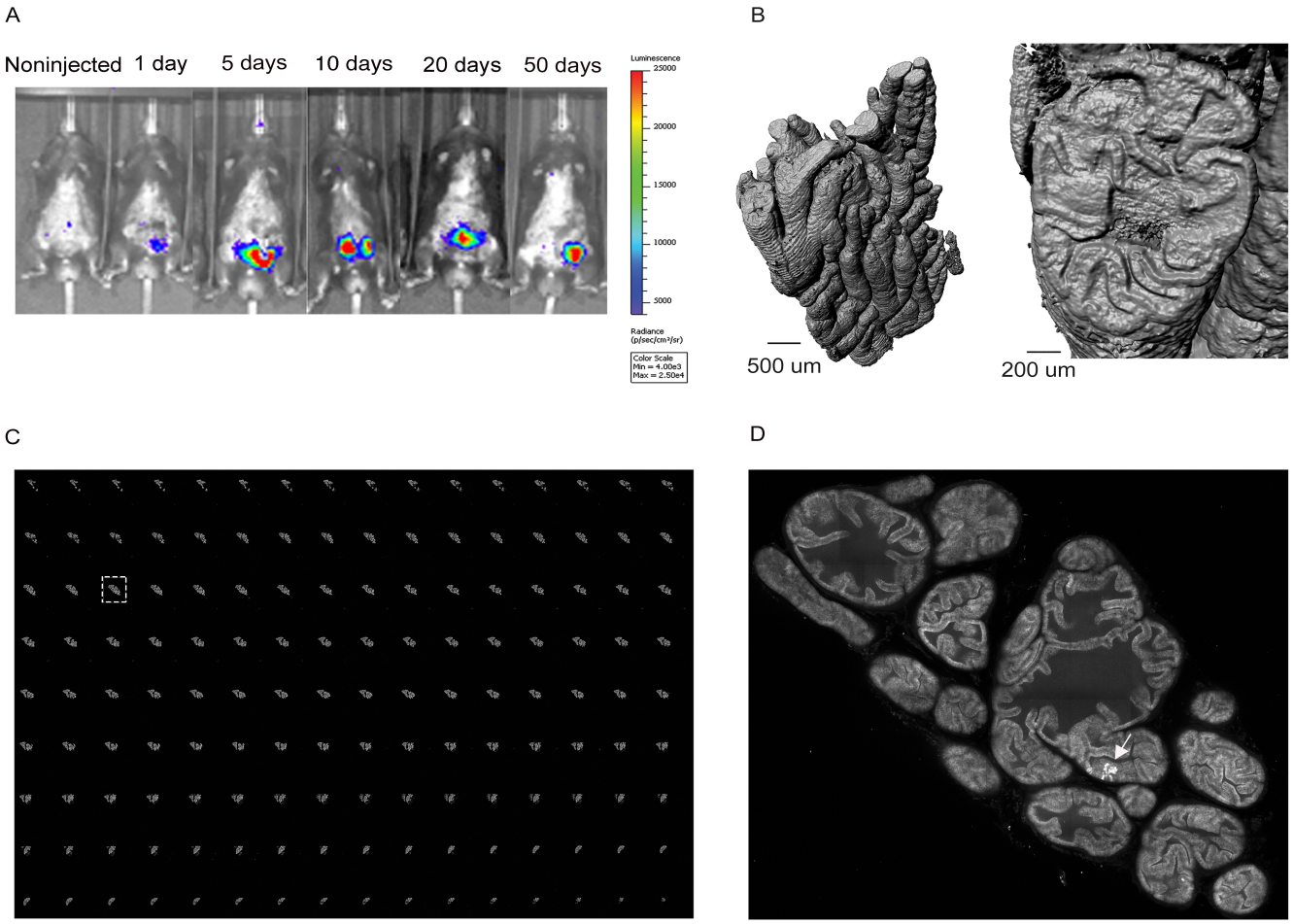

Figure S1. Bioluminescence and STPT imaging of eTOM RapidCaP mice, related to Figure 1. (A) RapidCaP system: after surgical injection of Cre/Luciferase lentivirus (LV-Cre/Luci) into the anterior prostate gland, the of the disease can be monitored by live bioluminescence imaging (BLI), as shown at 1, 5-, 10-, 20-, and 50-days post-injection. The luciferase scale is shown on the right.

(B) 3D view showing the whole-prostate and enlarged image of a top view from the same gland.

(C) Serial 145-section montage of the mouse prostate from the apex to the base imaged at 1 um x 1 um x 50 um x-y-z resolution (the section in the white square is shown in D).

(D) Complete 2D view of a transverse prostate section showing the identification of individual epithelial tdT+ cells at 10 days post-injection.

Figure S2

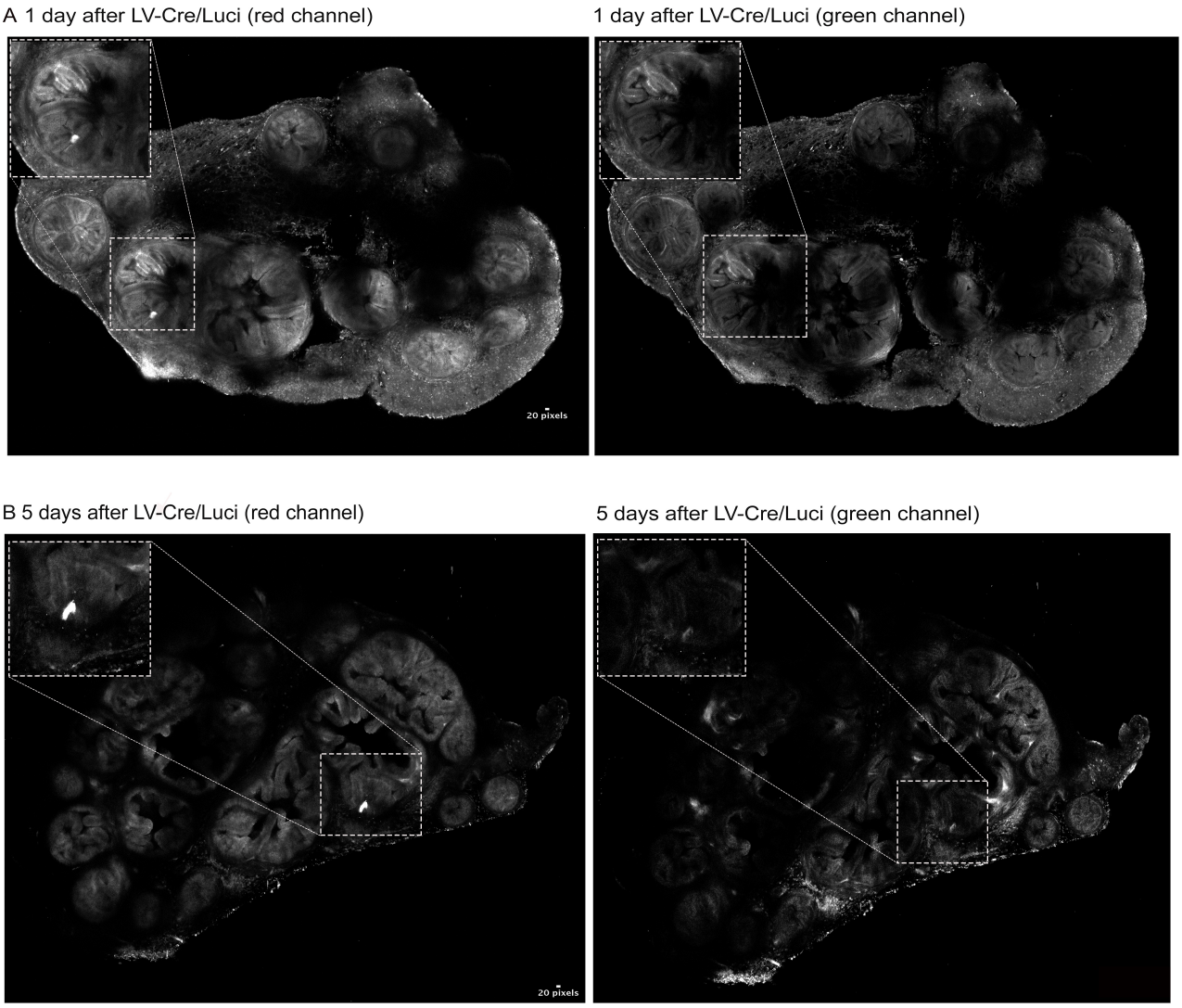

Figure S2. Days 1 and 5 in a time course of PC initiation and proliferation in the eTOM Rapid-CaP mice, related to Figure 2. (A) Transverse section of the prostate at 1-day post-injection with individual cells or group of maximum 10 tdT+ epithelial cells detected in the signal channel (red channel; left panel). The specificity of the signal is confirmed by the lack of signal in the autofluorescence background channel also collected during STPT imaging (green channel; right panel) (number of mice analyzed n: 7).
(B) Transverse section of the prostate at 5-days post-injection showing a small cluster with more than 10 tdT+ epithelial cells, which is similar as seen at 1-day post-injection, in the signal channel (red channel; left panel). The specificity of the signal is again confirmed by the lack of signal in the background channel (green channel; right panel) (number of mice analyzed n: 5).

Figure S3

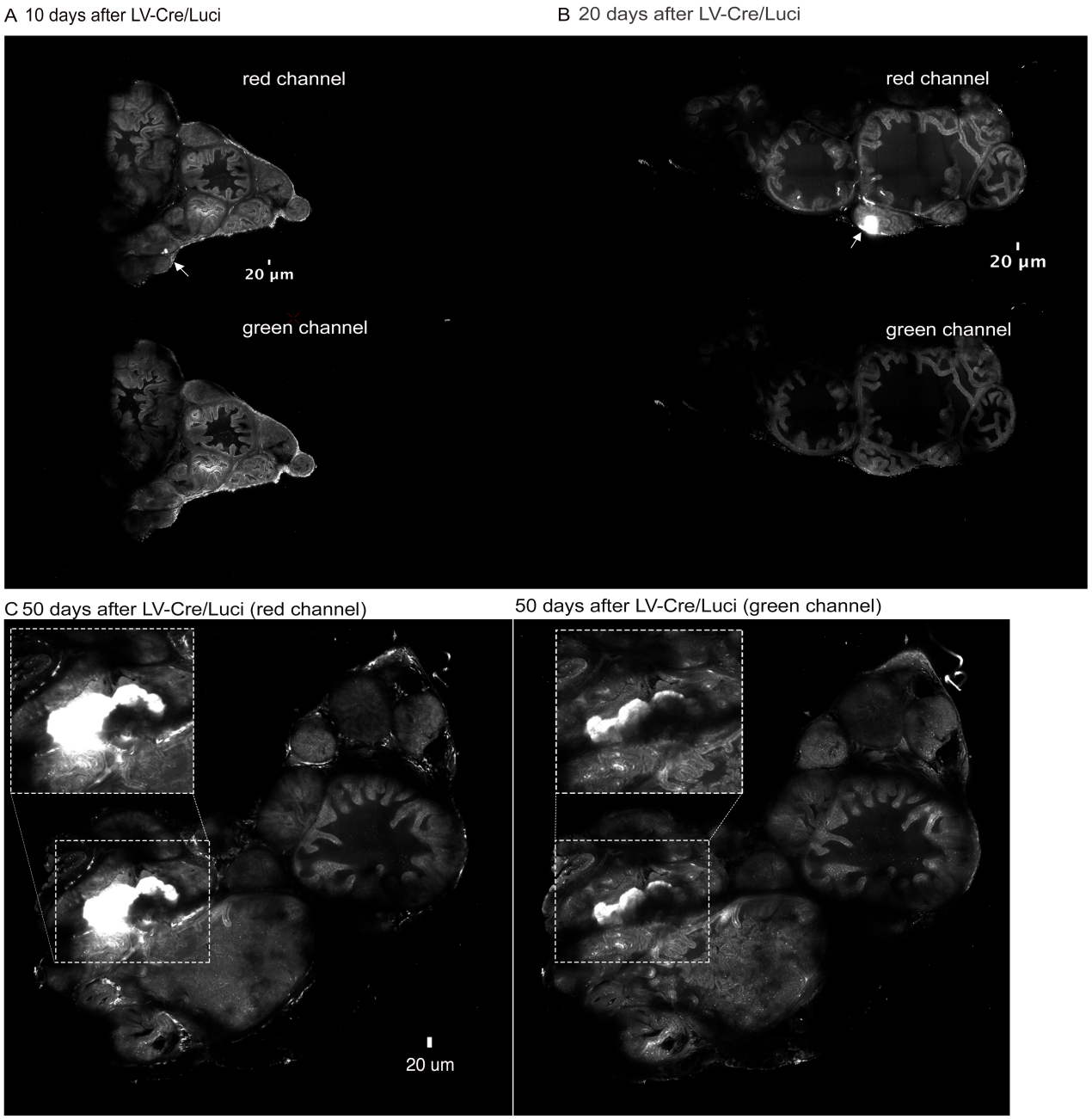

Figure S3. Days 10, 20 and 50 in a time course of PC initiation and proliferation in eTOM Rapid-CaP animals, related to Figure 2. (A) Transverse section of prostate at 10-days post-injection with a small cluster of tdT+ epithelial cells detected in the signal channel (red channel; left panel) (number of mice analyzed: n: 7).

(B) Transverse section of prostate at 20-days post-injection with a larger cluster of tdT+ epithelial cells detected in the signal channel (red channel; left panel) (number of mice analyzed: n: 5).

(C) Transverse section of prostate at 50-days post-injection with a larger cluster of tdT+ epithelial cells detected in the signal channel (red channel; left panel). (A-C) The specificity of the signal is confirmed by its lack in the background channel collected during STPT imaging (green channel; right panel), except 50 days when channel bleed is registered at the sites of highest red intensity (number of mice analyzed n: 5).

Figure S4

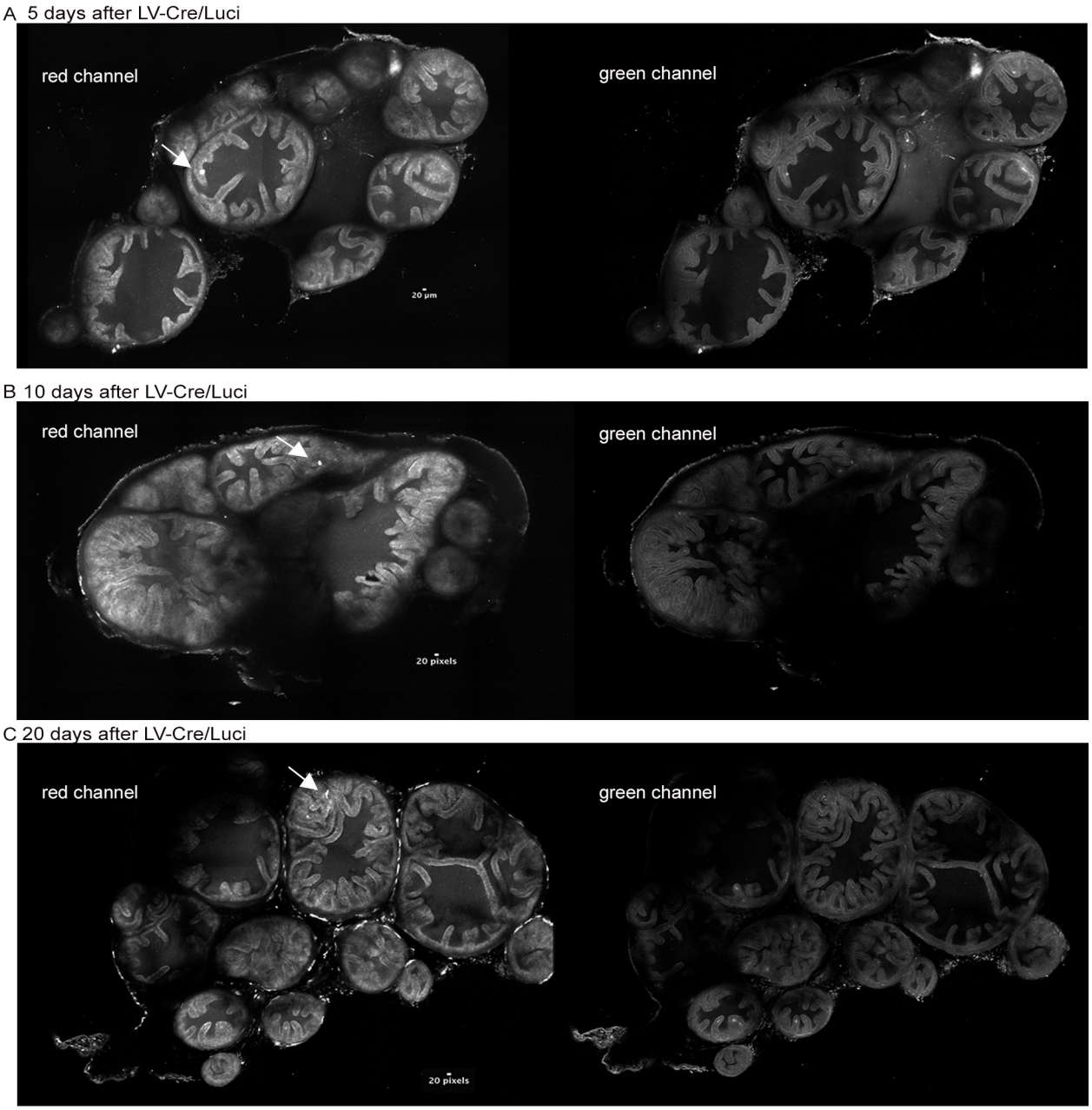

Figure S4. Absence of tdT+ cell expansion in wt Pten/Trp53 Ai9(RCL-tdT) lsl-tdTomato-reporter mice, related to Figure 2. (A-C) Transverse section of prostate at 5 (A), 10 (B) and 20 (C) days post-injection clusters of tdT+ epithelial cells detected in the signal channel (red channel; left panel) (number of mice analyzed 5 days n: 5, 10 days n: 7, 20 days n: 5). The specificity of the signals is confirmed by its lack in the background channel collected during STPT imaging (green channel; right panel).

Figure S5

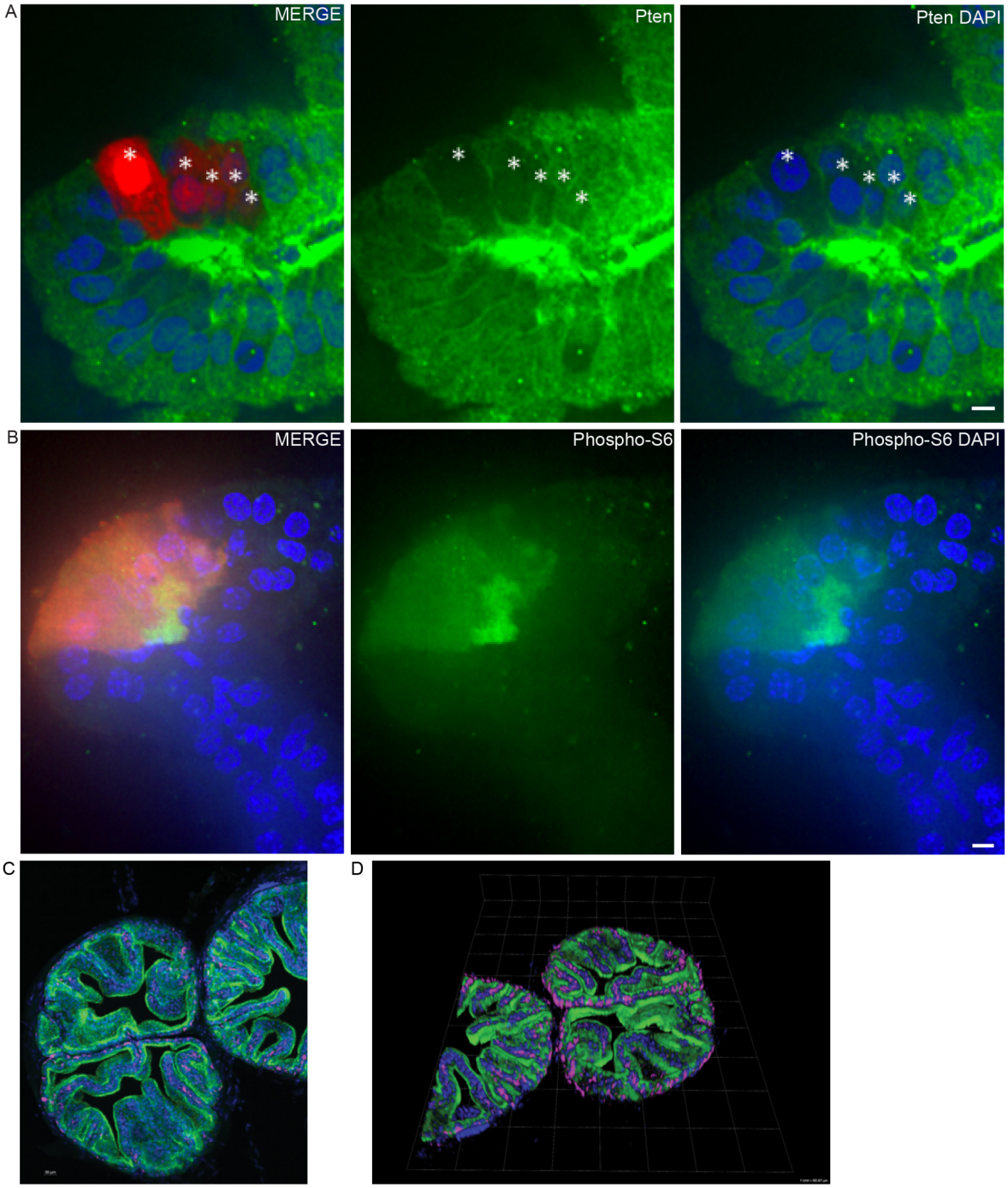

Figure S5. Pten expression and phospho-S6 pathway activation in the mouse prostate after 10 days post-injection and immunostainings of 50 um prostate sections from STPT, related to Figure 2.
Immunofluorescence using Pten antibody confirms the specific recombination between the lentivirus and PtenloxP/loxP-Trp53loxP/loxP-Ai9(RCL-tdT). (A) Asterisks show five epithelial cells that are tdTomato positive, and they are negative for Pten protein marker (Scale bar, 5 um).
(B) Phospho-S6 pathway activation is downstream of Pten protein. In both cases, we applied deconvolution with Imaris 9.7.2 and then maximum projection.
(C) and (D). CK8 staining in wild-type prostate shows normal morphology. CK5 staining in wild-type prostate shows normal morphology. In both images, the nucleus of epithelial cells are marked with DAPI (Scale bar, 10 um).

Figure S6

A

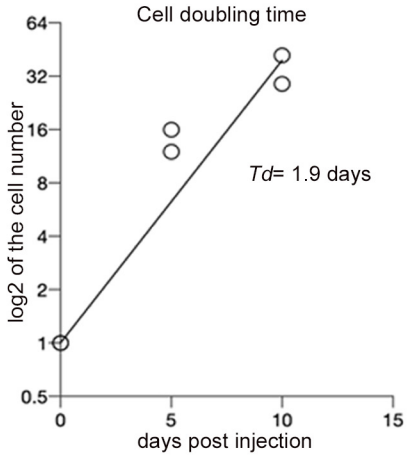

B 1 day tdTomato⁺/CK8⁺

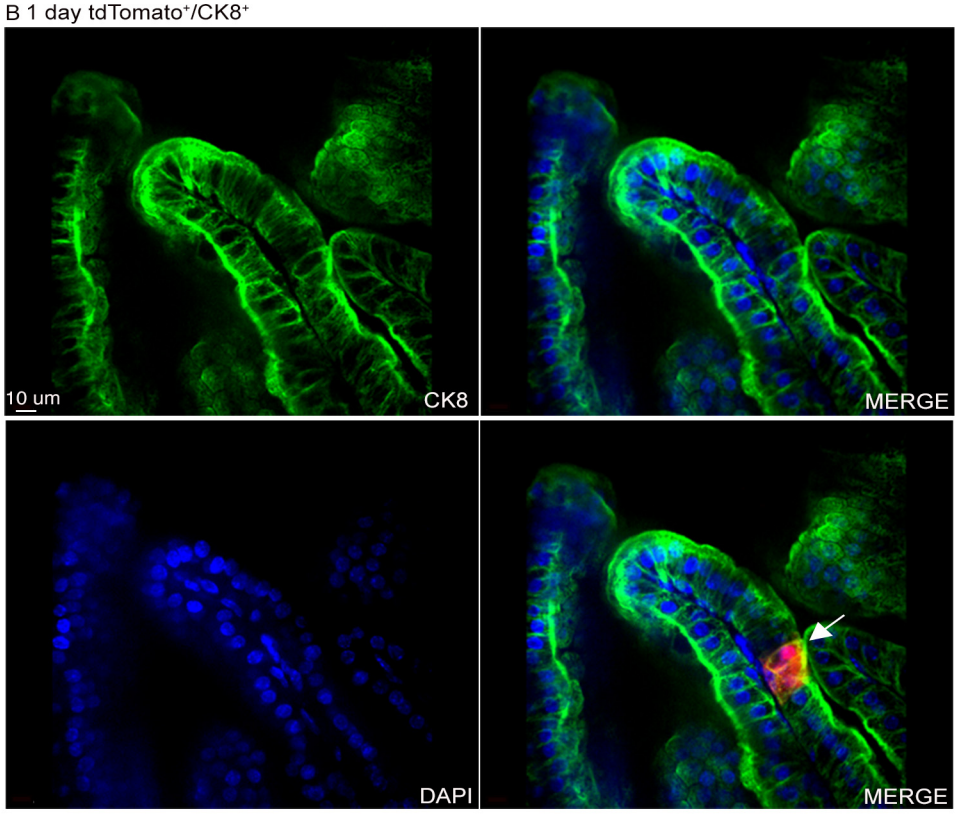

C 10 days tdTomato⁺ /E-Cad

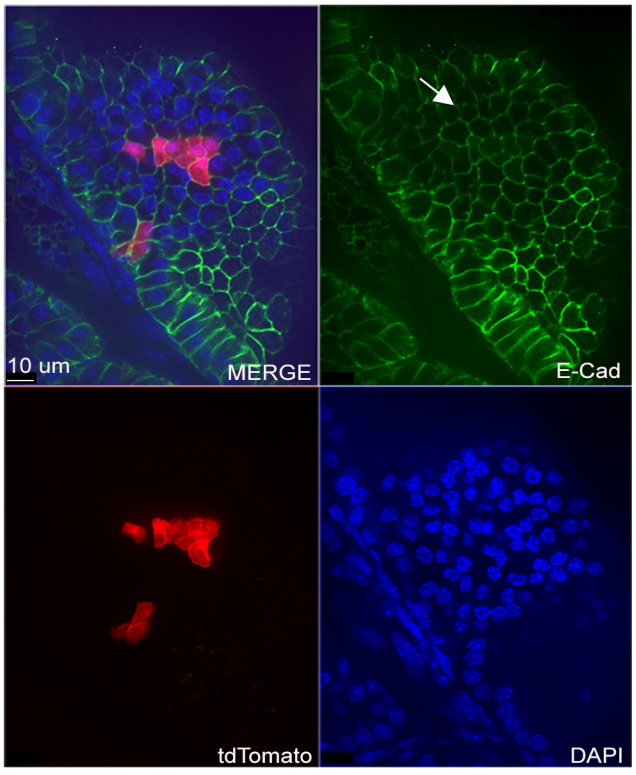

D 20 days tdTomato⁺/E-Cad

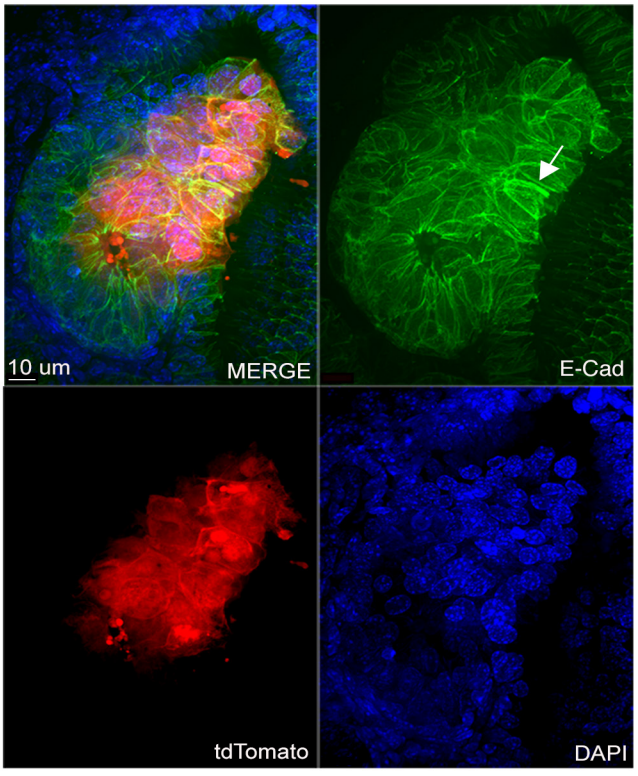

Figure S6. Quantification of the proliferation rate in early lesion based on cell counts and immunostaining-based analysis of the cellular morphology in the prostate foci, related to Figure 2. (A) Manual cell counts of tdT+ cells in mouse STPT prostate sections of animals after 5 (number of mice analyzed n: 2) and 10 days post-injection (number of mice analyzed n: 2).
(B-C) Immunofluorescence labeling with anti-CK8 and E-Cad antibodies shows normal epithelial architecture of the prostate gland in the region comprising tdT+ cells at 1- and 10-days post-injection.
(D) In contrast, at 20 days post-injection clear morphological changes are visible in a larger focus comprising tdT+ cells.

Figure S7

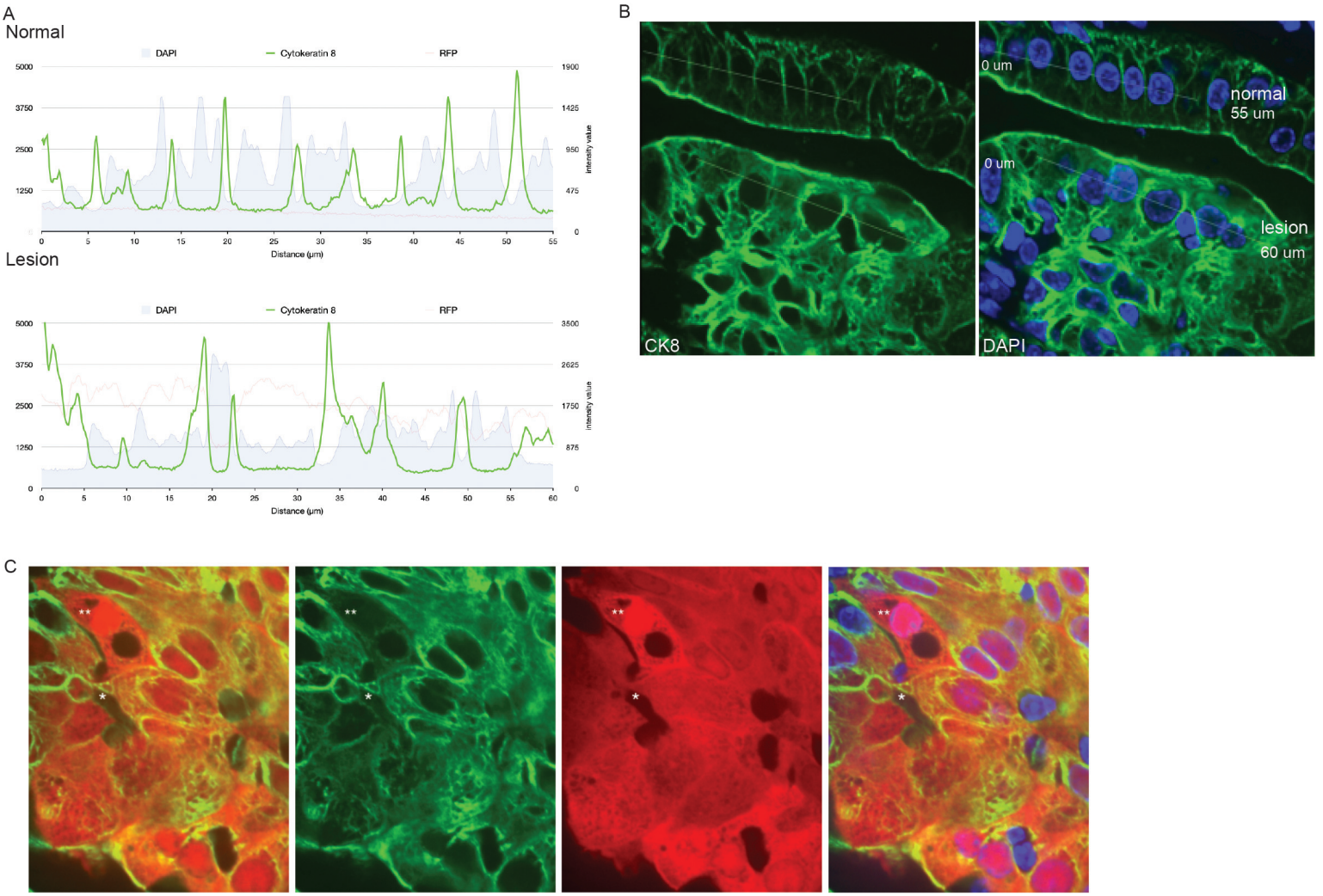

Figure S7. Quantification of the fluorescence intensity in epithelial cells and cell morphology at 20 days post-injection corresponding to CK8 expression, related to Figure 2. (A) Peaks of fluorescence intensity in a normal region of the gland (top) and in an area with tdT+ cells (bottom) showing traces for DAPI nuclei labeling (light blue), keratin labeling (green line) and tdT (RFP – red line). Notice the regular spacing of nuclei and keratin signal in normal tissue which is strongly disrupted in the cancer tissue.
(B) Image of immunofluorescence of prostate tissue using Ck8 antibody covering two areas analyzed.
(C) Changes in CK8 and cell lesion in prostate at 20 days post-injection. The anti-CK8 immunostaining of a dense focal site of tdT+ cells revealed areas of rare putative cell-free space (*) and nearby cancer cells with low CK8 expression (**).

Figure S8

A 20 days post-injection

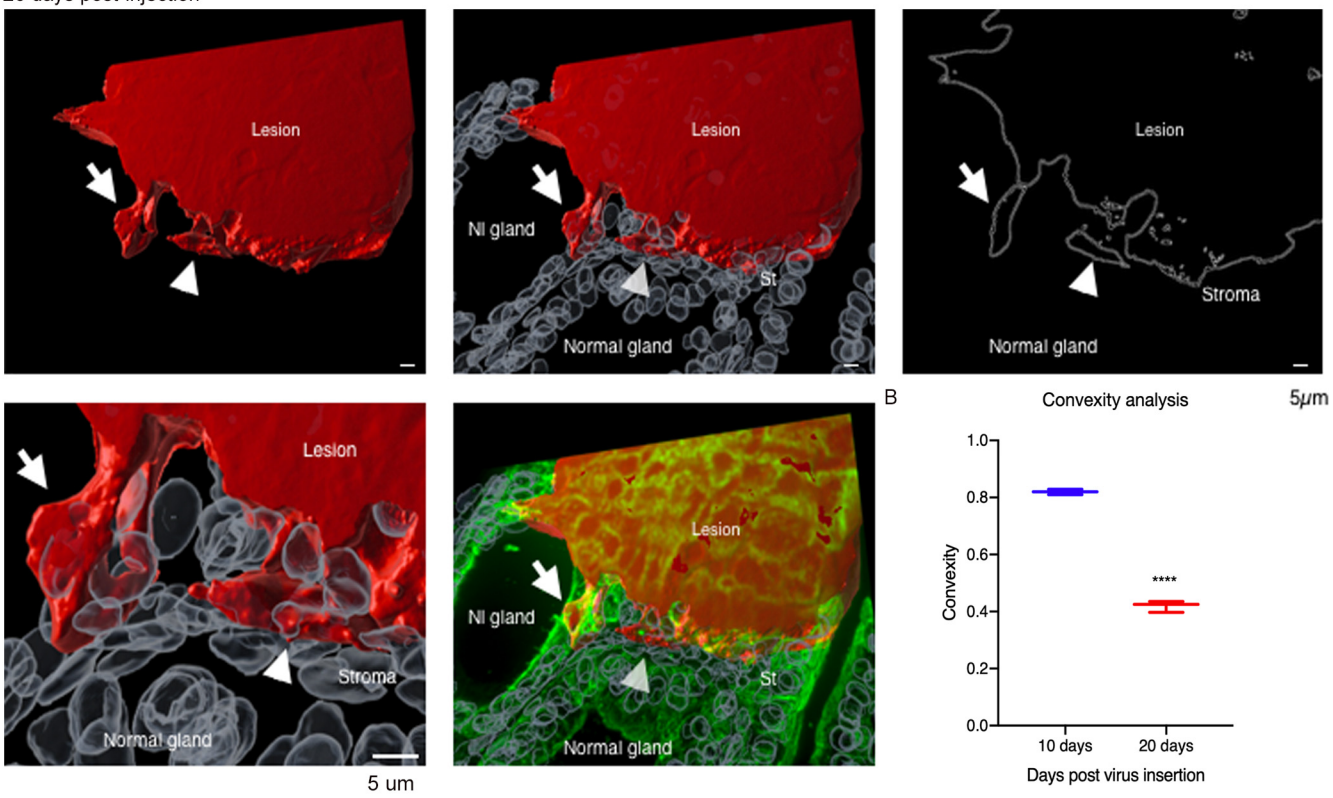

B

C 50 days post-injection

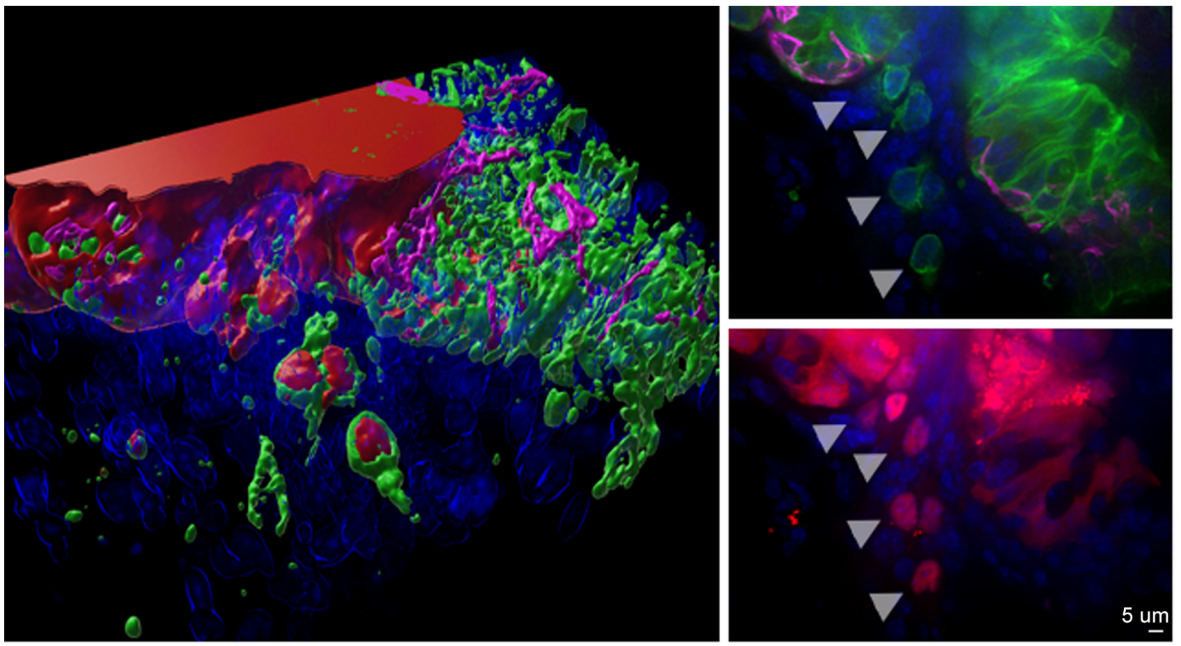

Figure S8. 3D images of the tdT+ foci at 20- and 50-days post-injection, related to Figure 2.
(A) 3D reconstruction and volume rendering of confocal images done on the agarose slice from a single focal lesion (red volume and its outline) at 20 days post-injection. Epithelial cells are marked by Cytokeratin 8 antibody (green) and tumor cell protrusions into stroma are show indicated by white arrows.
(B) Quantification and statistical analysis of convexity, a measure for spherical morphology (=1.0) of the tumor-stroma boundary in lesions from 10- and 20-days post-injection shown in Figure 2E-F ($p \leq 0.0001$).
(C) Analysis of a lesion (red) at 50 days post-injection and reconstructed as in (A) shows invasive epithelial tumor cells (white head arrows) escaping from the tumor. Cytokeratin 8 (green) and Cytokeratin 5 (purple) are also shown. Note the rearrangement of cytokeratin 8 in escaping tumor cells (Scale bar, 5 um).

Figure S9

A

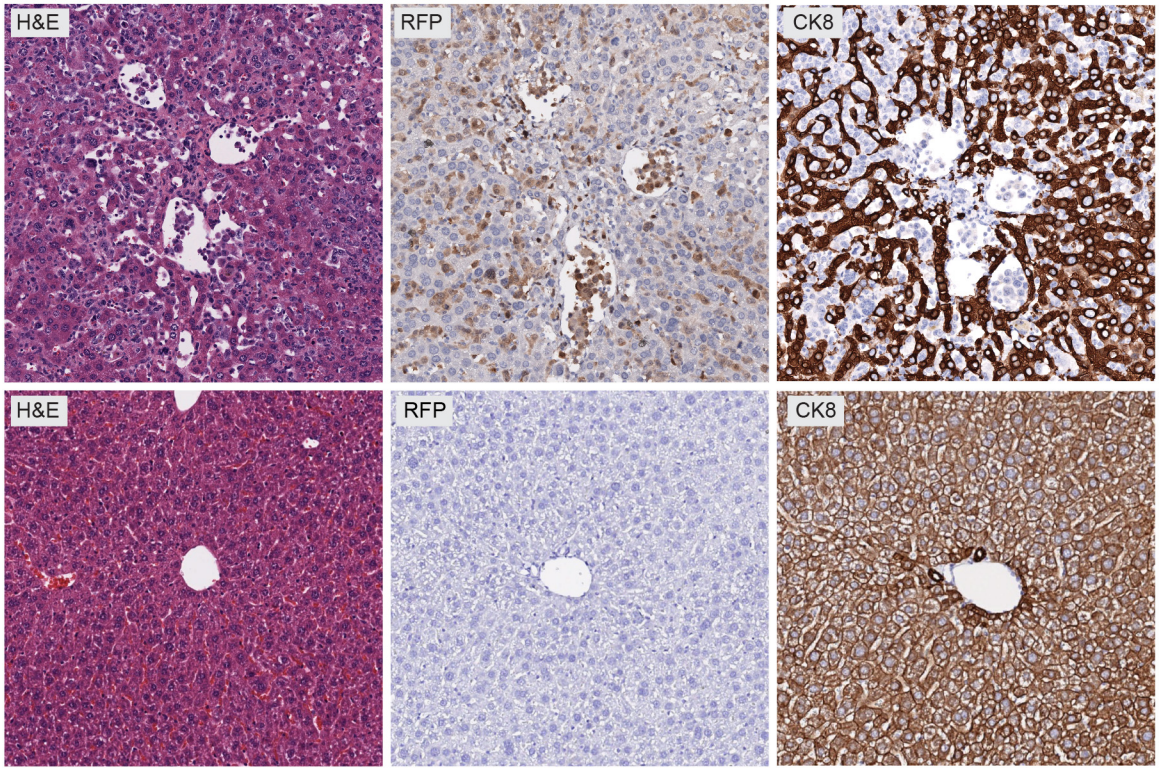

B

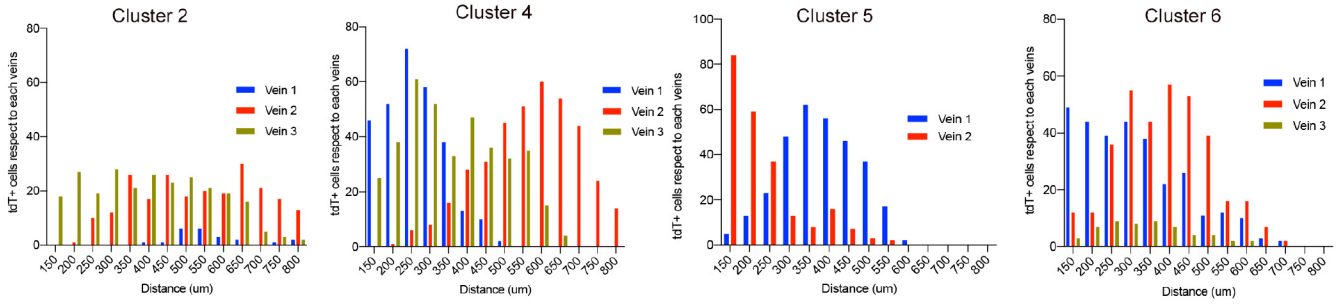

C

Range of the tdT+ cells	Cluster 1	Cluster 2	Cluster 3	Cluster 4	Cluster 5	Cluster 6	Cluster 7
Distant to the vain (closer - farther tdT+ cell)	30 um- 632 um	52 um - 822 um	71 um- 407 um	37 um - 483 um	49 um - 540 um	28 um - 685 um	30 um - 742 um

Figure S9. Immunohistochemistry in mouse liver metastatic FFPE-based sections and histograms of td+ cells distribution in the liver, related to Figure 3. (A) FFPE-based staining of late stage metastasis bearing liver tissue from eTOM RapidCaP mouse (15 months p.i.) confirms low-density of tdTomato+ cells, seen using STPT-confocalanalysis (see Cho et al., Methods 2015). As shown in the figure, tdT+ cells are seen dispersed in liver tissue, showing checkered staining for the hepatocyte marker Ck8 and the tumor marker tdTomato, H&E staining, we identify the metastatic cells in the 5 um liver section from the eTOM RapidCaP mouse model. Additionally, using RFP antibody, we detect the metastatic cells that are expressing tdTomato. Finally, we confirmed that these cells don't express the cytokeratin-8 marker, and it is consistent with the data previously shown in Figure 3F (scale bar, 100 um).
(B) Histograms for clusters 2, 4, 5, and 6 in the mouse liver. Distance ranges of tdT+ cells to the three main veins closer to each cluster.
(C) Table shows the shortest and farther distance for the tdT+ cells in the 7 metastatic clusters in the liver.

Figure S10

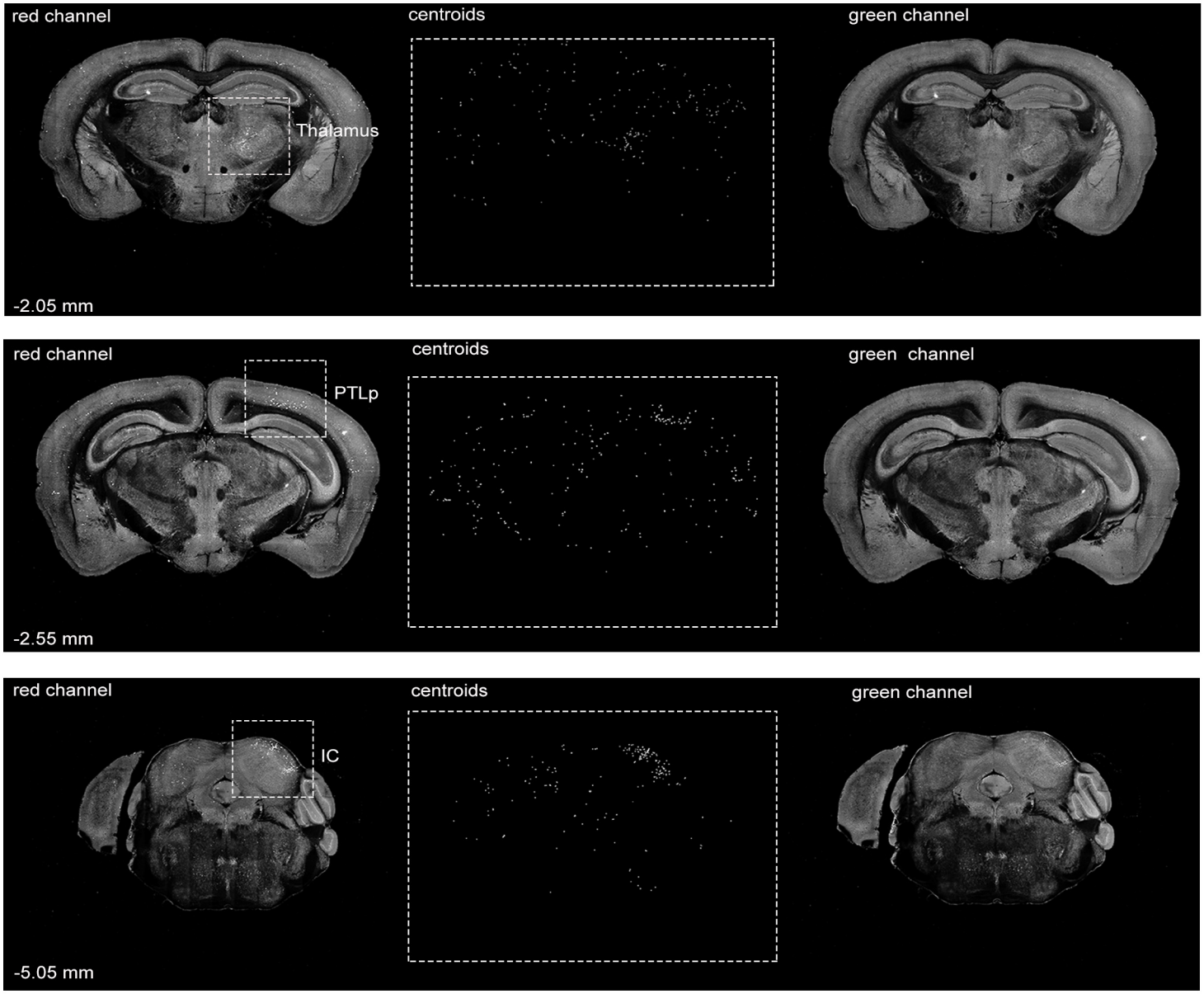

Figure S10. Additional examples of tdT+ metastatic cells detected in the brain, relate to Figure 4. Coronal brain sections from STPT imaging showing metastatic tdT+ cells in the thalamus, posterior parietal association area (PTLp), and inferior colliculus (IC). The specificity of the signal is confirmed by its lack in the background channel collected during STPT imaging (green channel; right panel).

Figure S11

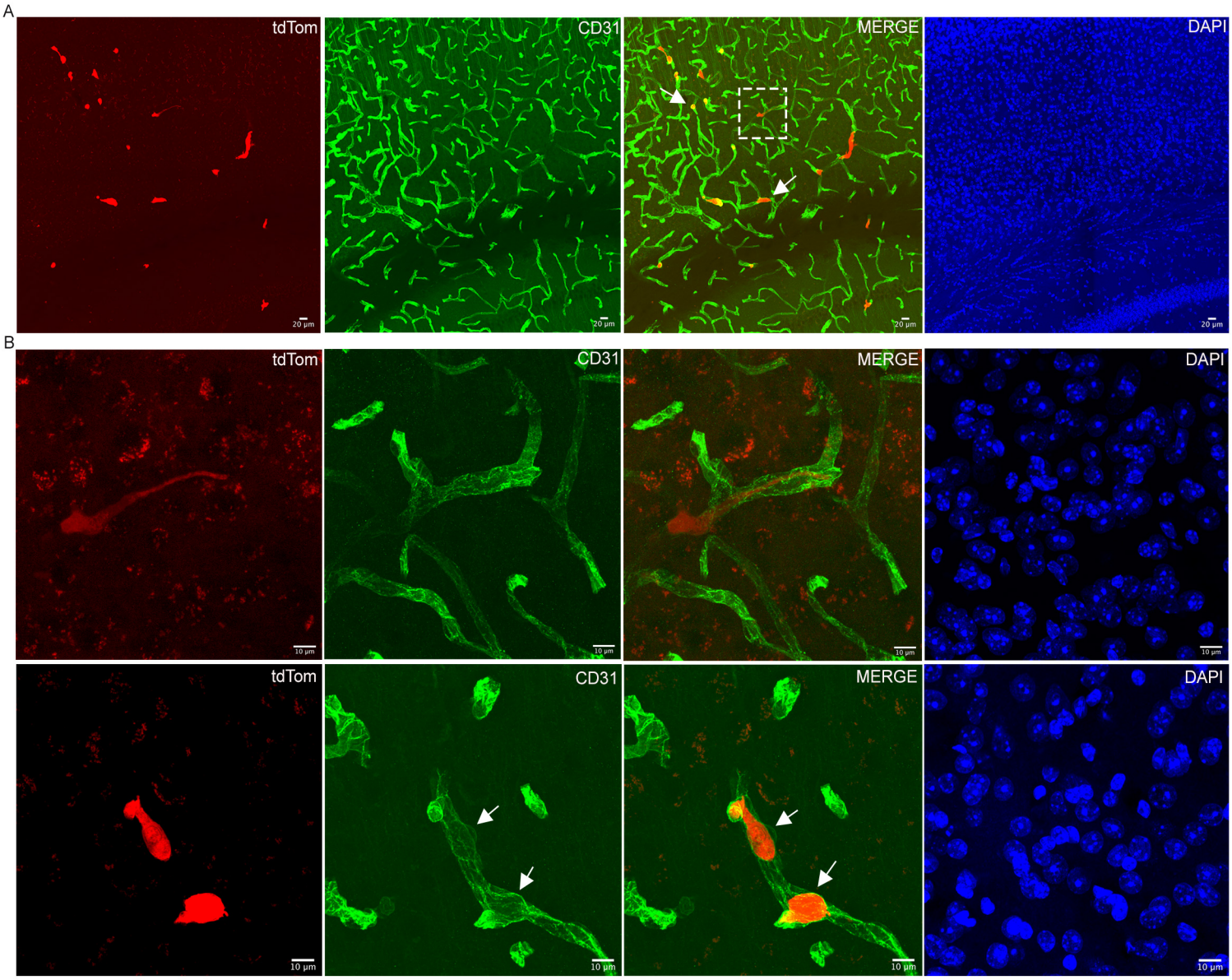

Figure S11. Immunostaining in brain sections with tdT + cells in combination with CD31 marker to detect endothelial blood vessel cells, related to Figure 4. (A) Immunofluorescence in coronal brain sections from STPT showing metastatic tdT+ cells and anti-CD31 vasculature labeling (green) in the somatosensory cortex area (scale bar, 10 um).
(B) Higher magnification view from the same area shows metastatic tdT+ cells located in the intravascular space. A second example of tdT + cells detected in intravascular space (white arrow) and possible expansion in the blood vessels (number of mice analyzed n: 2) (scale bar, 10 um).

Figure S12

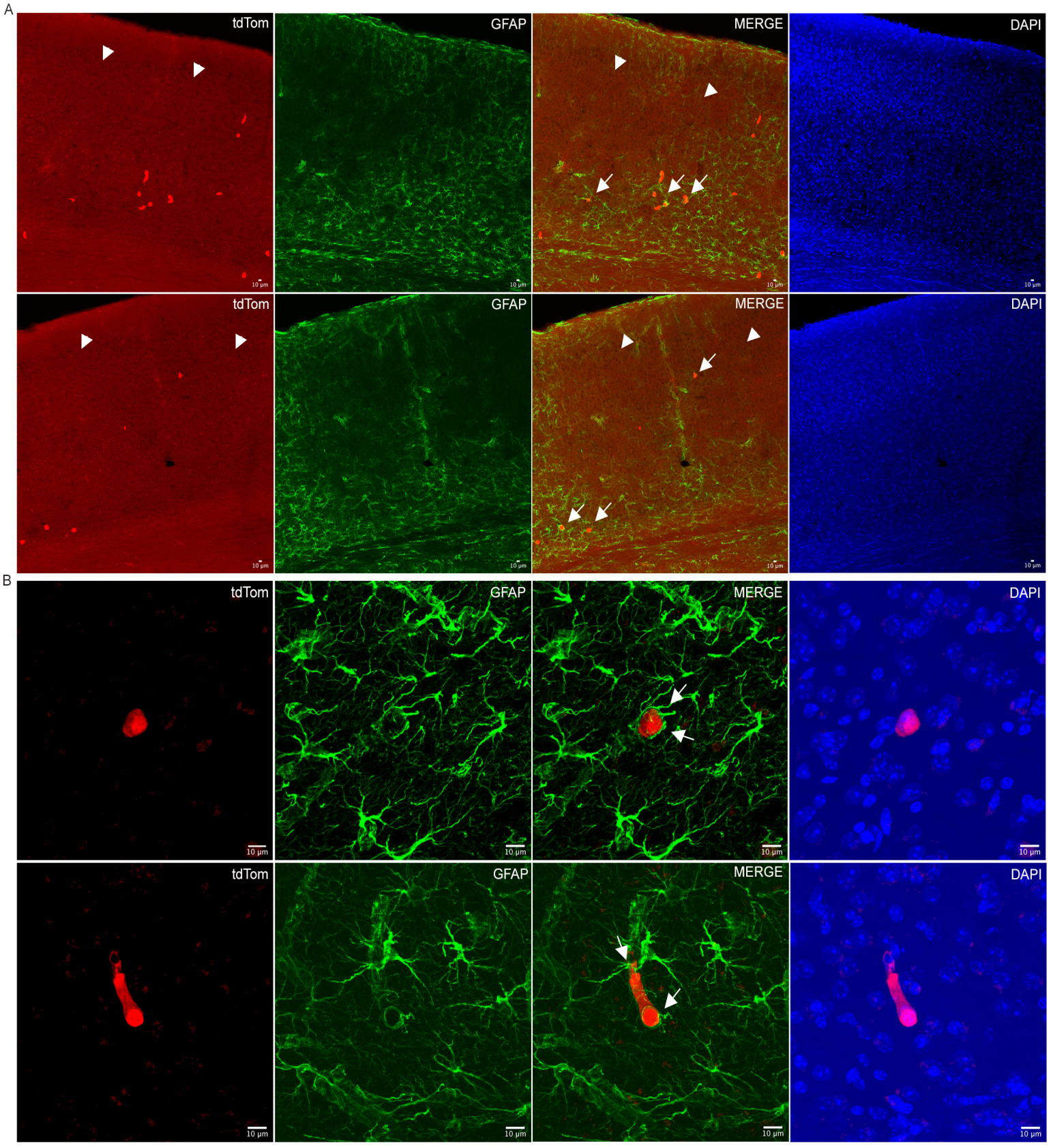
A
tdTom
GFAP
MERGE
DAPI
tdTom
GFAP
MERGE
DAPI
B
tdTom
GFAP
MERGE
DAPI
tdTom
GFAP
MERGE
DAPI

Figure S12. Immunostaining with anti-GFAP antibody to visualize astrocytic activation in coronal brain sections, related to Figure 4. (A) Sections from STPT show metastatic tdT+ cells in the deep layers of the somatosensory cortex that also comprise higher labeling of astrocytes labeled with anti-GFAP antibodies (green) (white arrow) (Scale bar, 10 um).
(B) Two examples in higher magnification showing astrocyte protrusions that appear to surround the space around metastatic tdT+ cells (white arrow) (number of mice analyzed n: 2 mice) (Scale bar, 10 um).

Figure S13

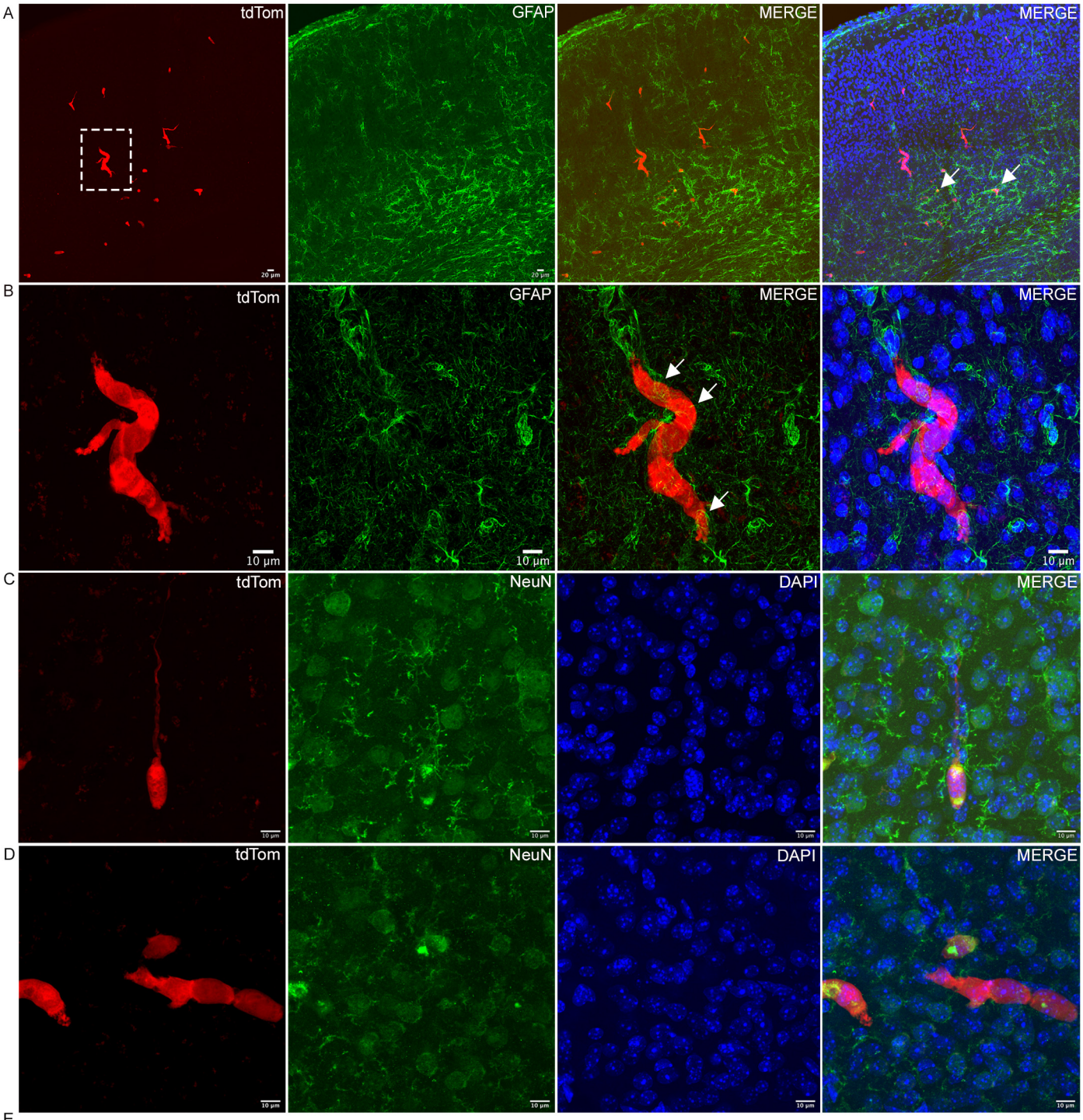
A
tdTom
GFAP
MERGE
MERGE
20 µm
B
tdTom
GFAP
MERGE
MERGE
10 µm
C
tdTom
NeuN
DAPI
MERGE
D
tdTom
NeuN
DAPI
MERGE
E
****
Volume (um3)
1000
800
600
400
200
0
Neuron NeuN+
tdTom cells from cortex

Figure S13. Immunostaining of astrocytes using the GFAP antibody and quantification of tdT+ cell nuclei in the brain section compared with neurons, related to Figure 4. (A) and (B) High-resolution example of tdT+ cells groups (around 7 cells) and in-line organization (Scale bar, 10 um).
(C) tdT+ cell with a large protuberance and neighboring neurons marked with NeuN antibody (green), with DAPI labeling of all cell nuclei.
(D) An additional example of multiple nearby tdT+ cells (Scale bar, 10 um).
(E) A graphic showing the volume (um3) of the nuclei of neurons and tdT+ cells (number of mice analyzed n: 2 mice, 10 tdT+ cells, and 40 neurons).